$R$esearch in
$A$stronomy and
$A$strophysics

# Effect of solar wind plasma parameters on space weather

Balveer S. Rathore, Dinesh C. Gupta and Subhash C. Kaushik

School of Study in Physics, Jiwaji University, Gwalior, Madhya Pradesh, India;
*balveer_singhra@yahoo.co.in*

**Abstract** Today's challenge for space weather research is to quantitatively predict the dynamics of the magnetosphere from measured solar wind and interplanetary magnetic field (IMF) conditions. Correlative studies between geomagnetic storms (GMSs) and the various interplanetary (IP) field/plasma parameters have been performed to search for the causes of geomagnetic activity and develop models for predicting the occurrence of GMSs, which are important for space weather predictions. We find a possible relation between GMSs and solar wind and IMF parameters in three different situations and also derived the linear relation for all parameters in three situations. On the basis of the present statistical study, we develop an empirical model. With the help of this model, we can predict all categories of GMSs. This model is based on the following fact: the total IMF $B_{\text{total}}$ can be used to trigger an alarm for GMSs, when sudden changes in total magnetic field $B_{\text{total}}$ occur. This is the first alarm condition for a storm's arrival. It is observed in the present study that the southward $B_z$ component of the IMF is an important factor for describing GMSs. A result of the paper is that the magnitude of $B_z$ is maximum neither during the initial phase (at the instant of the IP shock) nor during the main phase (at the instant of Disturbance storm time (Dst) minimum). It is seen in this study that there is a time delay between the maximum value of southward $B_z$ and the Dst minimum, and this time delay can be used in the prediction of the intensity of a magnetic storm two-three hours before the main phase of a GMS. A linear relation has been derived between the maximum value of the southward component of $B_z$ and the Dst, which is $\text{Dst} = (-0.06) + (7.65)B_z + t$. Some auxiliary conditions should be fulfilled with this, for example the speed of the solar wind should, on average, be 350 km s$^{-1}$ to 750 km s$^{-1}$, plasma $\beta$ should be low and, most importantly, plasma temperature should be low for intense storms. If the plasma temperature is less than $0.5 \times 10^6$ K then the Dst value will be greater than the predicted value of Dst or if temperature is greater than $0.5 \times 10^6$ K then the Dst value will be less (some nT).

**Key words:** solar wind — geomagnetic storms (GMSs) — interplanetary magnetic field (IMF)

## 1 INTRODUCTION

As is well known, geomagnetic storms (GMSs) generally occur due to abnormal conditions in the interplanetary magnetic field (IMF) and emissions from solar wind plasma caused by various solar

phenomenon (Akasofu 1983; Joselyn & McIntosh 1981), like coronal mass ejections (CMEs) and solar flares. The study of these worldwide disturbances associated with Earth's magnetic field are important for understanding the dynamics of the solar-terrestrial environment, because such storms can be the cause of life threatening power outrages, satellite damage, communication failures and navigational problems (Joselyn & McIntosh 1981; Lakhina 1994; Gonzalez et al. 1994). To explain the dynamics of GMSs in terms of enhanced solar wind magnetospheric coupling processes, various researchers have proposed a number of suggestions. Dungey (1961) suggested that magnetic reconnection occurs in the daytime magnetopause between the Earth's magnetic field and the southward component of the IMF. After reconnection, when the field lines are swept back in the magnetotail, a neutral point is formed through which the charged particles gain entry into the magnetosphere. High-energy particles rush towards the Earth but are deflected into circular orbits around the Earth forming a ring current, which causes considerable reductions in the geomagnetic field strength. These reductions in the Earth's magnetic field strength are measured by the Disturbance storm time (Dst) index. Low-energy particles spiral around the stretched geomagnetic field lines and collide with the terrestrial atmosphere in the polar region, causing enhanced aurora. Dst, Kp, Ap and AE indices are the four most commonly used geomagnetic activity indices. In the present paper, we use the Dst index. The geomagnetic environment is strongly affected by the Sun and its activities such as solar flares, active prominences, CMEs, corotating interaction regions, the solar wind stream from coronal holes, etc., which are responsible for GMSs. In terms of time sequence, GMSs can be described as having three phases: the initial, main and recovery phases. The initial phase may be gradual or represented by a sudden change in the Dst index (the Dst index increases to a positive value) called a sudden commencement. The main phase of a storm is said to begin when the Dst index starts decreasing from its sudden commencement value and, after some time, it assumes a negative value and ends when it decreases to its minimum value. The recovery phase, usually the longest one, is characterized by a return of the Dst index to its pre-sudden-commencement value. During a GMS, the solar wind and CMEs coming from the Sun and the Earth's magnetosphere are connected, giving rise to several changes in both the interplanetary (IP) and terrestrial environment (Gonzalez et al. 1999). In general, the solar wind's ability to penetrate into near-Earth space is thought to rely on the magnetic alignment of the IMFs. As the solar wind streams from the Sun toward the day side of Earth, its magnetic fields connect up to those of Earth, resulting in a sudden and dramatic reconfiguration or reconnection of the field lines. According to earlier findings, this is most efficient when the IMF is aligned southward – opposite to the northward alignment of Earth's magnetic field. The temporary tangling of the field lines creates ideal conditions for magnetic reconnection, allowing large amounts of plasma and magnetic energy to be transferred from the solar wind to the magnetosphere.

## 2 SELECTION CRITERIA AND DATA COLLECTION

Disturbances in the geomagnetic field are caused by fluctuations in the solar wind impinging on Earth. These disturbances may be limited to the high-latitude polar region, unless the IMF carried by the solar wind has long periods (several hours or more) of a southward component ($B_z < 0$) with large magnitudes (Joselyn & McIntosh 1981; Lakhina 1994; Gonzalez et al. 1994). The occurrence of such a period continuously stresses the magnetosphere, causing the magnetic field disturbance to reach the equatorial region. The degree of equatorial magnetic field deviation is usually given by the Dst index (Sugiura 1964). This is the hourly average of the deviation from the horizontal (H) component of the magnetic field measured by several ground stations in mid to low latitudes. Dst $= 0$ means no deviation from the quiet condition and Dst $\leq -50$ nT means magnetic storms are occurring (Lakhina 1994; Gonzalez et al. 1994).

A list of magnetic storms, based on Dst indices, has been compiled for the present study by using data provided by the World Data Center for Geomagnetism, Kyoto, Japan through its website (*http/:wdc.kugi.kyoto-u.ac.jp/dstdir*). The IMF and solar wind parameters

are taken from the OMNIweb database, maintained by the National Geophysical Data Center (*www.omniweb.gsfc.nasa.gov*), and compiled for this study for the period 1996–2007. The period under study refers to solar cycle 23. In the present study, a set of 200 GMSs with Dst $\leq -50$ nT has been acquired, and is shown in Table 1.

**Table 1**  A List of Cases Showing Dst $\leq -50$ nT for GMSs

| S. No. | Start Date | Time (UT) | End Date | Time (UT) | Peak Date | Time (UT) | Dst (nT) |
|---|---|---|---|---|---|---|---|
| 1 | 13/01/1996 | (06:00) | 13/01/1996 | (19:00) | 13/01/1996 | (11:00) | −90 |
| 2 | 23/10/1996 | (01:00) | 23/10/1996 | (11:00) | 23/10/1996 | (05:00) | −105 |
| 3 | 10/01/1997 | (09:00) | 10/01/1997 | (18:00) | 10/01/1997 | (10:00) | −78 |
| 4 | 10/02/1997 | (07:00) | 10/02/1997 | (21:00) | 10/02/1997 | (11:00) | −68 |
| 5 | 11/04/1997 | (02:00) | 11/04/1997 | (09:00) | 11/04/1997 | (05:00) | −82 |
| 6 | 21/04/1997 | (19:00) | 22/04/1997 | (09:00) | 21/04/1997 | (24:00) | −107 |
| 7 | 15/05/1997 | (09:00) | 15/05/1997 | (24:00) | 15/05/1997 | (13:00) | −115 |
| 8 | 27/05/1997 | (02:00) | 27/05/1997 | (11:00) | 27/05/1997 | (05:00) | −73 |
| 9 | 08/06/1997 | (23:00) | 09/06/1997 | (14:00) | 09/06/1997 | (04:00) | −84 |
| 10 | 03/09/1997 | (21:00) | 04/09/1997 | (11:00) | 03/09/1997 | (23:00) | −98 |
| 11 | 01/10/1997 | (11:00) | 01/10/1997 | (24:00) | 01/10/1997 | (16:00) | −98 |
| 12 | 10/10/1997 | (20:00) | 11/10/1997 | (19:00) | 11/10/1997 | (04:00) | −130 |
| 13 | 07/11/1997 | (02:00) | 07/11/1997 | (18:00) | 07/11/1997 | (05:00) | −110 |
| 14 | 10/11/1997 | (02:00) | 10/11/1997 | (07:00) | 10/11/1997 | (03:00) | −54 |
| 15 | 22/11/1997 | (13:00) | 22/11/1997 | (18:00) | 22/11/1997 | (16:00) | −75 |
| 16 | 23/11/1997 | (01:00) | 24/11/1997 | (04:00) | 23/11/1997 | (13:00) | −108 |
| 17 | 07/1/1998 | (03:00) | 07/1/1998 | (12:00) | 07/1/1998 | (05:00) | −77 |
| 18 | 17/02/1998 | (20:00) | 18/02/1998 | (11:00) | 18/02/1998 | (01:00) | −100 |
| 19 | 10/03/1998 | (17:00) | 12/03/1998 | (09:00) | 10/03/1998 | (21:00) | −116 |
| 20 | 21/03/1998 | (15:00) | 21/03/1998 | (23:00) | 21/03/1998 | (16:00) | −85 |
| 21 | 26/04/1998 | (16:00) | 26/04/1998 | (22:00) | 26/04/1998 | (18:00) | −63 |
| 22 | 02/05/1998 | (14:00) | 02/05/1998 | (22:00) | 02/05/1998 | (18:00) | −85 |
| 23 | 03/05/1998 | (04:00) | 03/05/1998 | (09:00) | 03/05/1998 | (07:00) | −69 |
| 24 | 04/05/1998 | (01:00) | 06/05/1998 | (24:00) | 04/05/1998 | (06:00) | −205 |
| 25 | 26/06/1998 | (03:00) | 26/06/1998 | (09:00) | 26/06/1998 | (05:00) | −101 |
| 26 | 06/08/1998 | (09:00) | 070/8/1998 | (24:00) | 06/08/1998 | (12:00) | −138 |
| 27 | 27/08/1998 | (01:00) | 29/08/1998 | (08:00) | 27/08/1998 | (10:00) | −155 |
| 28 | 31/08/1998 | (11:00) | 31/08/1998 | (20:00) | 31/08/1998 | (12:00) | −60 |
| 29 | 25/09/1998 | (03:00) | 25/09/1998 | (24:00) | 25/09/1998 | (10:00) | −207 |
| 30 | 26/09/1998 | (14:00) | 26/09/1998 | (22:00) | 26/09/1998 | (18:00) | −75 |
| 31 | 07/10/1998 | (19:00) | 08/10/1998 | (04:00) | 07/10/1998 | (23:00) | −70 |
| 32 | 19/10/1998 | (05:00) | 20/10/1998 | (06:00) | 19/10/1998 | (16:00) | −112 |
| 33 | 20/10/1998 | (18:00) | 21/10/1998 | (12:00) | 20/10/1998 | (23:00) | −71 |
| 34 | 06/11/1998 | (15:00) | 06/11/1998 | (20:00) | 06/11/1998 | (19:00) | −60 |
| 35 | 07/11/1998 | (14:00) | 08/11/1998 | (14:00) | 08/11/1998 | (07:00) | −149 |
| 36 | 09/11/1998 | (16:00) | 10/11/1998 | (15:00) | 09/11/1998 | (16:00) | −131 |
| 37 | 13/11/1998 | (07:00) | 15/11/1998 | (05:00) | 13/11/1998 | (19:00) | −128 |
| 38 | 11/12/1998 | (08:00) | 11/12/1998 | (19:00) | 11/12/1998 | (16:00) | −69 |
| 39 | 13/01/1999 | (18:00) | 14/01/1998 | (21:00) | 13/01/1999 | (24:00) | −112 |
| 40 | 18/02/1999 | (06:00) | 20/02/1999 | (03:00) | 18/02/1999 | (18:00) | −123 |
| 41 | 01/03/1999 | (17:00) | 02/03/1999 | (10:00) | 01/03/1999 | (20:00) | −95 |
| 42 | 17/04/1999 | (02:00) | 17/04/1999 | (10:00) | 17/04/1999 | (08:00) | −91 |
| 43 | 23/08/1999 | (01:00) | 23/08/1999 | (08:00) | 23/08/1999 | (01:00) | −66 |
| 44 | 23/08/1999 | (14:00) | 23/08/1999 | (19:00) | 23/08/1999 | (16:00) | −63 |
| 45 | 13/09/1999 | (01:00) | 13/09/1999 | (20:00) | 13/09/1999 | (03:00) | −72 |
| 46 | 14/09/1999 | (04:00) | 14/09/1999 | (09:00) | 14/09/1999 | (08:00) | −65 |
| 47 | 16/09/1999 | (05:00) | 16/09/1999 | (17:00) | 16/09/1999 | (09:00) | −67 |
| 48 | 22/09/1999 | (22:00) | 23/09/1999 | (24:00) | 22/09/1999 | (24:00) | −173 |
| 49 | 27/09/1999 | (16:00) | 27/09/1999 | (24:00) | 27/09/1999 | (19:00) | −64 |
| 50 | 10/10/1999 | (15:00) | 10/10/1999 | (24:00) | 10/10/1999 | (19:00) | −67 |
| 51 | 15/10/1999 | (02:00) | 15/10/1999 | (07:00) | 15/10/1999 | (06:00) | −67 |

**Table 1** — *Continued*

| S. No. | Start Date | Time (UT) | End Date | Time (UT) | Peak Date | Time (UT) | Dst (nT) |
|---|---|---|---|---|---|---|---|
| 52 | 22/10/1999 | (02:00) | 24/10/1999 | (17:00) | 22/10/1999 | (07:00) | −237 |
| 53 | 07/11/1999 | (13:00) | 07/11/1999 | (22:00) | 07/11/1999 | (16:00) | −67 |
| 54 | 08/11/1999 | (13:00) | 08/11/1999 | (24:00) | 08/11/1999 | (15:00) | −73 |
| 55 | 13/11/1999 | (01:00) | 13/11/1999 | (12:00) | 13/11/1999 | (09:00) | −69 |
| 56 | 13/11/1999 | (14:00) | 14/11/1999 | (18:00) | 13/11/1999 | (23:00) | −106 |
| 57 | 13/12/1999 | (08:00) | 13/12/1999 | (17:00) | 13/12/1999 | (10:00) | −85 |
| 58 | 11/01/2000 | (20:00) | 12/01/2000 | (08:00) | 11/01/2000 | (22:00) | −81 |
| 59 | 22/01/2000 | (21:00) | 23/01/2000 | (17:00) | 23/01/2000 | (01:00) | −97 |
| 60 | 12/02/2000 | (10:00) | 13/02/2000 | (01:00) | 12/02/2000 | (12:00) | −133 |
| 61 | 13/02/2000 | (03:00) | 13/02/2000 | (16:00) | 13/02/2000 | (09:00) | −57 |
| 62 | 14/02/2000 | (13:00) | 14/02/2000 | (24:00) | 14/02/2000 | (14:00) | −67 |
| 63 | 06/04/2000 | (19:00) | 08/04/2000 | (19:00) | 07/04/2000 | (01:00) | −288 |
| 64 | 10/04/2000 | (01:00) | 10/04/2000 | (17:00) | 10/04/2000 | (06:00) | −66 |
| 65 | 24/04/2000 | (14:00) | 24/04/2000 | (19:00) | 24/04/2000 | (15:00) | −61 |
| 66 | 17/05/2000 | (03:00) | 17/05/2000 | (10:00) | 17/05/2000 | (06:00) | −92 |
| 67 | 24/05/2000 | (04:00) | 25/05/2000 | (21:00) | 24/05/2000 | (09:00) | −147 |
| 68 | 08/06/2000 | (18:00) | 090/6/2000 | (03:00) | 08/06/2000 | (20:00) | −90 |
| 69 | 15/07/2000 | (20:00) | 17/07/2000 | (18:00) | 16/07/2000 | (01:00) | −301 |
| 70 | 20/07/2000 | (04:00) | 21/07/2000 | (04:00) | 20/07/2000 | (10:00) | −93 |
| 71 | 11/08/2000 | (01:00) | 11/08/2000 | (19:00) | 11/08/2000 | (07:00) | −106 |
| 72 | 12/08/2000 | (04:00) | 13/08/2000 | (18:00) | 12/08/2000 | (10:00) | −235 |
| 73 | 17/09/2000 | (22:00) | 19/09/2000 | (07:00) | 17/09/2000 | (24:00) | −201 |
| 74 | 19/09/2000 | (12:00) | 20/09/2000 | (05:00) | 19/09/2000 | (15:00) | −77 |
| 75 | 30/09/2000 | (13:00) | 30/09/2000 | (18:00) | 30/09/2000 | (15:00) | −76 |
| 76 | 03/10/2000 | (04:00) | 03/10/2000 | (18:00) | 3/10/2000 | (10:00) | −75 |
| 77 | 04/10/2000 | (09:00) | 06/10/2000 | (19:00) | 5/10/2000 | (14:00) | −182 |
| 78 | 14/10/2000 | (01:00) | 14/10/2000 | (24:00) | 14/10/2000 | (15:00) | −107 |
| 79 | 29/10/2000 | (01:00) | 30/10/2000 | (03:00) | 29/10/2000 | (04:00) | −127 |
| 80 | 06/11/2000 | (15:00) | 07/11/2000 | (19:00) | 06/11/2000 | (22:00) | −159 |
| 81 | 10/11/2000 | (11:00) | 11/11/2000 | (04:00) | 10/11/2000 | (13:00) | −96 |
| 82 | 27/11/2000 | (01:00) | 27/11/2000 | (08:00) | 27/11/2000 | (02:00) | −80 |
| 83 | 28/11/2000 | (15:00) | 30/11/2000 | (12:00) | 29/11/2000 | (14:00) | −119 |
| 84 | 19/03/2001 | (18:00) | 21/03/2001 | (24:00) | 20/03/2001 | (14:00) | −149 |
| 85 | 23/03/2001 | (10:00) | 23/03/2001 | (23:00) | 23/03/2001 | (17:00) | −75 |
| 86 | 31/03/2001 | (06:00) | 02/04/2001 | (19:00) | 31/03/2001 | (09:00) | −387 |
| 87 | 09/04/2001 | (01:00) | 09/04/2001 | (11:00) | 09/04/2001 | (07:00) | −63 |
| 88 | 11/04/2001 | (18:00) | 14/04/2001 | (05:00) | 11/04/2001 | (24:00) | −271 |
| 89 | 18/04/2001 | (05:00) | 19/04/2001 | (07:00) | 18/04/2001 | (07:00) | −114 |
| 90 | 22/04/2001 | (12:00) | 23/04/2001 | (16:00) | 22/04/2001 | (16:00) | −102 |
| 91 | 09/05/2001 | (17:00) | 10/05/2001 | (11:00) | 10/05/2001 | (02:00) | −76 |
| 92 | 17/08/2001 | (20:00) | 18/08/2001 | (06:00) | 17/08/2001 | (22:00) | −105 |
| 93 | 26/09/2001 | (01:00) | 26/09/2001 | (19:00) | 26/09/2001 | (02:00) | −102 |
| 94 | 01/10/2001 | (01:00) | 04/10/2001 | (23:00) | 01/10/2001 | (09:00) | −148 |
| 95 | 12/10/2001 | (07:00) | 12/10/2001 | (22:00) | 12/10/2001 | (13:00) | −71 |
| 96 | 21/10/2001 | (19:00) | 24/10/2001 | (12:00) | 21/10/2001 | (22:00) | −187 |
| 97 | 28/10/2001 | (05:00) | 29/10/2001 | (23:00) | 28/10/2001 | (12:00) | −157 |
| 98 | 01/11/2001 | (01:00) | 02/11/2001 | (04:00) | 01/11/2001 | (11:00) | −106 |
| 99 | 05/11/2001 | (22:00) | 08/11/2001 | (14:00) | 06/11/2001 | (07:00) | −292 |
| 100 | 24/11/2001 | (08:00) | 26/11/2001 | (17:00) | 24/11/2001 | (17:00) | −221 |
| 101 | 05/02/2002 | (20:00) | 05/02/2002 | (24:00) | 05/02/2002 | (21:00) | −82 |
| 102 | 06/02/2002 | (01:00) | 06/02/2002 | (19:00) | 06/02/2002 | (04:00) | −73 |
| 103 | 01/03/2002 | (01:00) | 01/03/2002 | (12:00) | 01/03/2002 | (02:00) | −71 |
| 104 | 24/03/2002 | (04:00) | 25/03/2002 | (06:00) | 24/03/2002 | (10:00) | −100 |
| 105 | 17/04/2002 | (16:00) | 21/04/2002 | (07:00) | 20/04/2002 | (09:00) | −149 |
| 106 | 11/05/2002 | (16:00) | 12/05/2002 | (17:00) | 11/05/2002 | (20:00) | −110 |
| 107 | 14/05/2002 | (18:00) | 15/05/2002 | (07:00) | 15/05/2002 | (01:00) | −65 |
| 108 | 23/05/2002 | (12:00) | 24/05/2002 | (24:00) | 23/05/2002 | (18:00) | −109 |

**Table 1** — *Continued*

| S. No. | Start Date | Time (UT) | End Date | Time (UT) | Peak Date | Time (UT) | Dst (nT) |
|---|---|---|---|---|---|---|---|
| 109 | 02/08/2002 | (02:00) | 02/08/2002 | (10:00) | 02/08/2002 | (06:00) | −102 |
| 110 | 020/8/2002 | (21:00) | 03/08/2002 | (06:00) | 02/08/2002 | (23:00) | −69 |
| 111 | 20/08/2002 | (01:00) | 20/08/2002 | (07:00) | 20/08/2002 | (01:00) | −71 |
| 112 | 20/08/2002 | (21:00) | 21/08/2002 | (20:00) | 21/08/2002 | (07:00) | −106 |
| 113 | 04/09/2002 | (04:00) | 04/09/2002 | (24:00) | 04/09/2002 | (06:00) | −109 |
| 114 | 07/09/2002 | (18:00) | 09/09/2002 | (10:00) | 08/09/2002 | (01:00) | −181 |
| 115 | 10/09/2002 | (01:00) | 10/09/2002 | (24:00) | 10/09/2002 | (23:00) | −82 |
| 116 | 11/09/2002 | (15:00) | 12/09/2002 | (08:00) | 11/09/2002 | (23:00) | −90 |
| 117 | 01/10/2002 | (10:00) | 03/10/2002 | (09:00) | 01/10/2002 | (17:00) | −176 |
| 118 | 03/10/2002 | (12:00) | 06/10/2002 | (11:00) | 04/10/2002 | (09:00) | −146 |
| 119 | 06/10/2002 | (17:00) | 10/10/2002 | (19:00) | 07/10/2002 | (08:00) | −115 |
| 120 | 14/10/2002 | (10:00) | 15/10/2002 | (02:00) | 14/10/2002 | (14:00) | −100 |
| 121 | 15/10/2002 | (18:00) | 15/10/2002 | (24:00) | 15/10/2002 | (19:00) | −70 |
| 122 | 16/10/2002 | (20:00) | 17/10/2002 | (03:00) | 16/10/2002 | (21:00) | −63 |
| 123 | 24/10/2002 | (04:00) | 25/10/2002 | (21:00) | 24/10/2002 | (21:00) | −98 |
| 124 | 27/10/2002 | (14:00) | 28/10/2002 | (08:00) | 27/10/2002 | (16:00) | −65 |
| 125 | 02/11/2002 | (18:00) | 04/11/2002 | (24:00) | 03/11/2002 | (07:00) | −75 |
| 126 | 05/11/2002 | (04:00) | 05/11/2002 | (10:00) | 05/11/2002 | (05:00) | −60 |
| 127 | 21/11/2002 | (05:00) | 23/11/2002 | (08:00) | 21/11/2002 | (11:00) | −128 |
| 128 | 25/11/2002 | (13:00) | 25/11/2002 | (18:00) | 25/11/2002 | (13:00) | −54 |
| 129 | 27/11/2002 | (03:00) | 27/11/2002 | (12:00) | 27/11/2002 | (07:00) | −64 |
| 130 | 19/12/2002 | (16:00) | 20/12/2002 | (02:00) | 19/12/2002 | (21:00) | −72 |
| 131 | 20/12/2002 | (05:00) | 20/12/2002 | (09:00) | 20/12/2002 | (06:00) | −64 |
| 132 | 21/12/2002 | (01:00) | 21/12/2002 | (08:00) | 21/12/2002 | (04:00) | −75 |
| 133 | 23/12/2002 | (09:00) | 23/12/2002 | (16:00) | 23/12/2002 | (12:00) | −67 |
| 134 | 27/12/2002 | (05:00) | 27/12/2002 | (19:00) | 27/12/2002 | (07:00) | −68 |
| 135 | 02/02/2003 | (10:00) | 03/02/2003 | (05:00) | 02/02/2003 | (18:00) | −72 |
| 136 | 04/02/2003 | (08:00) | 04/02/2003 | (12:00) | 04/02/2003 | (10:00) | −74 |
| 137 | 04/03/2003 | (01:00) | 04/03/2003 | (10:00) | 04/03/2003 | (01:00) | −67 |
| 138 | 29/03/2003 | (03:00) | 29/03/2003 | (08:00) | 29/03/2003 | (05:00) | −62 |
| 139 | 29/03/2003 | (18:00) | 30/03/2003 | (02:00) | 29/03/2003 | (21:00) | −70 |
| 140 | 30/03/2003 | (19:00) | 31/03/2003 | (04:00) | 30/03/2003 | (23:00) | −76 |
| 141 | 31/03/2003 | (10:00) | 01/04/2003 | (08:00) | 31/03/2003 | (16:00) | −78 |
| 142 | 01/05/2003 | (01:00) | 01/05/2003 | (09:00) | 01/05/2003 | (01:00) | −78 |
| 143 | 10/05/2003 | (03:00) | 10/05/2003 | (15:00) | 10/05/2003 | (09:00) | −84 |
| 144 | 22/05/2003 | (01:00) | 22/05/2003 | (06:00) | 22/05/2003 | (03:00) | −73 |
| 145 | 29/05/2003 | (22:00) | 30/05/2003 | (17:00) | 29/05/2003 | (24:00) | −144 |
| 146 | 16/06/2003 | (16:00) | 16/06/2003 | (24:00) | 16/06/2003 | (23:00) | −68 |
| 147 | 17/06/2003 | (05:00) | 17/06/2003 | (16:00) | 17/06/2003 | (09:00) | −81 |
| 148 | 18/06/2003 | (06:00) | 19/06/2003 | (04:00) | 18/06/2003 | (10:00) | −141 |
| 149 | 11/07/2003 | (18:00) | 12/07/2003 | (17:00) | 12/07/2003 | (06:00) | −105 |
| 150 | 16/07/2003 | (10:00) | 16/07/2003 | (23:00) | 16/07/2003 | (14:00) | −90 |
| 151 | 18/08/2003 | (05:00) | 19/08/2003 | (12:00) | 19/08/2003 | (01:00) | −116 |
| 152 | 21/08/2003 | (17:00) | 22/08/2003 | (03:00) | 21/08/2003 | (24:00) | −68 |
| 153 | 14/10/2003 | (22:00) | 15/10/2003 | (13:00) | 14/10/2003 | (23:00) | −85 |
| 154 | 29/10/2003 | (08:00) | 01/11/2003 | (07:00) | 30/10/2003 | (23:00) | −383 |
| 155 | 04/11/2003 | (11:00) | 04/11/2003 | (18:00) | 04/11/2003 | (11:00) | −69 |
| 156 | 20/11/2003 | (14:00) | 22/11/2003 | (11:00) | 20/11/2003 | (21:00) | −422 |
| 157 | 22/11/2003 | (16:00) | 23/11/2003 | (12:00) | 22/11/2003 | (23:00) | −87 |
| 158 | 22/01/2004 | (13:00) | 23/01/2004 | (24:00) | 23/01/2004 | (14:00) | −130 |
| 159 | 25/01/2004 | (01:00) | 25/01/2004 | (24:00) | 25/01/2004 | (04:00) | −81 |
| 160 | 27/01/2004 | (01:00) | 27/01/2004 | (05:00) | 27/01/2004 | (02:00) | −62 |
| 161 | 11/02/2004 | (17:00) | 11/02/2004 | (24:00) | 11/02/2004 | (18:00) | −87 |
| 162 | 10/03/2004 | (01:00) | 10/03/2004 | (11:00) | 10/03/2004 | (06:00) | −78 |
| 163 | 03/04/2004 | (18:00) | 04/04/2004 | (09:00) | 04/04/2004 | (01:00) | −117 |
| 164 | 05/04/2004 | (19:00) | 05/04/2004 | (24:00) | 05/04/2004 | (20:00) | −62 |
| 165 | 17/07/2004 | (02:00) | 17/07/2004 | (08:00) | 17/07/2004 | (03:00) | −76 |

**Table 1** — *Continued*

| S. No. | Start Date | Time (UT) | End Date | Time (UT) | Peak Date | Time (UT) | Dst (nT) |
|---|---|---|---|---|---|---|---|
| 166 | 23/07/2004 | (01:00) | 23/07/2004 | (21:00) | 23/07/2004 | (03:00) | −99 |
| 167 | 25/07/2004 | (01:00) | 30/07/2004 | (06:00) | 27/07/2004 | (14:00) | −170 |
| 168 | 30/08/2004 | (15:00) | 31/08/2004 | (18:00) | 30/08/2004 | (23:00) | −117 |
| 169 | 07/11/2004 | (22:00) | 14/11/2004 | (14:00) | 08/11/2004 | (07:00) | −374 |
| 170 | 08/01/2005 | (01:00) | 08/01/2005 | (12:00) | 08/01/2005 | (03:00) | −93 |
| 171 | 18/01/2005 | (01:00) | 20/01/2005 | (07:00) | 18/01/2005 | (09:00) | −103 |
| 172 | 21/01/2005 | (21:00) | 23/01/2005 | (06:00) | 22/01/2005 | (06:00) | −97 |
| 173 | 18/02/2005 | (02:00) | 18/02/2005 | (08:00) | 18/02/2005 | (03:00) | −80 |
| 174 | 05/04/2005 | (01:00) | 05/04/2005 | (09:00) | 05/04/2005 | (05:00) | −70 |
| 175 | 08/05/2005 | (02:00) | 09/05/2005 | (09:00) | 08/05/2005 | (19:00) | −110 |
| 176 | 10/05/2005 | (02:00) | 10/05/2005 | (08:00) | 10/05/2005 | (04:00) | −55 |
| 177 | 15/05/2005 | (07:00) | 18/05/2005 | (09:00) | 15/05/2005 | (09:00) | −247 |
| 178 | 21/05/2005 | (05:00) | 21/05/2005 | (20:00) | 21/05/2005 | (07:00) | −63 |
| 179 | 30/05/2005 | (09:00) | 31/05/2005 | (08:00) | 30/05/2005 | (14:00) | −113 |
| 180 | 12/06/2005 | (20:00) | 13/06/2005 | (16:00) | 13/06/2005 | (01:00) | −106 |
| 181 | 23/06/2005 | (08:00) | 23/06/2005 | (20:00) | 23/06/2005 | (11:00) | −85 |
| 182 | 10/07/2005 | (14:00) | 11/07/2005 | (08:00) | 10/07/2005 | (21:00) | −92 |
| 183 | 12/07/2005 | (02:00) | 12/07/2005 | (09:00) | 12/07/2005 | (06:00) | −78 |
| 184 | 18/07/2005 | (04:00) | 18/07/2005 | (10:00) | 18/07/2005 | (07:00) | −67 |
| 185 | 24/08/2005 | (11:00) | 25/08/2005 | (24:00) | 24/08/2005 | (12:00) | −184 |
| 186 | 26/08/2005 | (03:00) | 26/08/2005 | (09:00) | 26/08/2005 | (08:00) | −58 |
| 187 | 31/08/2005 | (15:00) | 01/09/2005 | (13:00) | 31/08/2005 | (20:00) | −122 |
| 188 | 03/09/2005 | (03:00) | 03/09/2005 | (16:00) | 03/09/2005 | (06:00) | −63 |
| 189 | 04/09/2005 | (06:00) | 04/09/2005 | (11:00) | 04/09/2005 | (10:00) | −71 |
| 190 | 11/09/2005 | (06:00) | 14/09/2005 | (17:00) | 11/09/2005 | (11:00) | −139 |
| 191 | 15/09/2005 | (17:00) | 16/09/2005 | (13:00) | 15/09/2005 | (17:00) | −80 |
| 192 | 31/10/2005 | (18:00) | 31/10/2005 | (24:00) | 31/10/2005 | (21:00) | −74 |
| 193 | 05/04/2006 | (06:00) | 05/04/2006 | (21:00) | 05/04/2006 | (16:00) | −79 |
| 194 | 14/04/2006 | (06:00) | 14/04/2006 | (24:00) | 14/04/2006 | (10:00) | −98 |
| 195 | 20/08/2006 | (01:00) | 20/08/2006 | (07:00) | 20/08/2006 | (02:00) | −79 |
| 196 | 10/11/2006 | (01:00) | 10/11/2006 | (08:00) | 10/11/2006 | (02:00) | −63 |
| 197 | 30/11/2006 | (08:00) | 30/11/2006 | (15:00) | 30/11/2006 | (14:00) | −74 |
| 198 | 15/12/2006 | (01:00) | 16/12/2006 | (18:00) | 15/12/2006 | (06:00) | −159 |
| 199 | 24/03/2007 | (07:00) | 24/03/2007 | (15:00) | 24/03/2007 | (09:00) | −72 |
| 200 | 20/11/2007 | (18:00) | 20/11/2007 | (24:00) | 20/11/2007 | (21:00) | −59 |

## 3  RESULT AND DISCUSSION

The purpose of the present work is to study the problem of solar wind-magnetosphere coupling due to a geoeffective transient arising from solar/IP disturbances during solar cycle 23. In the 11 year period from 1996 to 2007, a total of 200 GMSs have been observed based on the Dst index. The Dst is derived from hourly horizontal magnetic variations recorded from a network of near-equatorial geomagnetic observatories. Variations in the horizontal component of the field on the ground are believed to be caused by changes in the global high-altitude equatorial ring current, which in turn depends on solar wind conditions. The list of magnetic storms with the minimum values of Dst $\leq -50$ nT during the 1996−2007 period was used for the present study of the interrelation between the Dst and solar wind/IMF parameters. The list of magnetic storms with Dst $\leq -50$ nT was completed with data on the following quantities: $B_{\text{total}}$, $B_y$, $B_z$, $V$, $E_y$, Density, Pressure, Plasma $\beta$ and Temperature as well as taking the indices of substorms AE. The correlation between IMF parameters and Dst for the study period has been investigated for different situations. Moreover, the correlation coefficients ($r$) and equation describing the linear regression line for all parameters

**Table 2** Correlation Coefficients between Dst and the IMF Parameters during Cycle 23 in All Three Conditions

| Geomagnetic Index | Solar wind and IMF parameter | Correlation Coefficient ($r$) for G1 | Correlation Coefficient ($r$) for G2 | Correlation Coefficient ($r$) for G3 |
|---|---|---|---|---|
| Dst (nT) | $B_{\text{total}}$ | $-0.71$ | $-0.72$ | $-0.80$ |
| Dst (nT) | $B_z$ | 0.22 | 0.22 | 0.82 |
| Dst (nT) | $B_y$ | $-0.07$ | $-0.16$ | $-0.42$ |
| Dst (nT) | Speed ($V$) | $-0.35$ | $-0.24$ | $-0.40$ |
| Dst (nT) | Density | $-0.14$ | $-0.24$ | $-0.31$ |
| Dst (nT) | Temperature | $-0.251$ | 0.009 | $-0.257$ |
| Dst (nT) | Pressure | $-0.30$ | $-0.48$ | $-0.50$ |
| Dst (nT) | Plasma $\beta$ | 0.13 | 0.24 | 0.41 |
| Dst (nT) | $E_y$ | $-0.16$ | $-0.38$ | $-0.86$ |
| Dst (nT) | AE | $-0.34$ | $-0.20$ | $-0.58$ |

with Dst have also been calculated for different sets of solar wind and IMF parameter data during cycle 23.

In the present work, all the parameters of solar wind are divided into three categories of data sets according to the phase of GMSs and according to the interaction of IMF with the Earth's magnetic field at different instants: (1) G1, taking IMF data at the instant of the IP shock or during the initial phase of the GMS. (2) G2, during the main phase of the storm or at the instant of Dst minimum. (3) G3, the maximum value of IMF and solar wind plasma parameter during the storm. The IP shock was determined by utilizing the criteria followed by Lindsay et al. (1994).

We have analyzed the impact of all parameters related to IMF and solar wind plasma on geomagnetic properties in all three situations, which has been discussed above in detail. The correlation coefficients have been calculated for all the given parameters with Dst, which are shown in Table 2.

### 3.1 Total Magnetic Field of IMF ($B_{\text{total}}$) vs. Dst

In order to solve problems in space weather and analyze the geoeffectiveness of the solar wind parameter, we have taken the total magnetic field $B_{\text{total}}$ corresponding to the Dst, according to the interaction of $B_{\text{total}}$ with Earth's magnetic field, as was discussed earlier. (1) G1, taking $B_{\text{total}}$ at the instant the IP shock or when the value of $B_{\text{total}}$ suddenly changes in the *in situ* measurement. (2) G2, during the main phase of the storm or at the instant of Dst minimum. (3) G3, the maximum value (peak) of $B_{\text{total}}$ during the storm.

Figure 1(a–c) shows the Dst and the corresponding value of IMF $B_{\text{total}}$ in three situations. Figure 1(a–b) depicts variations in the Dst index and the corresponding value of $B_{\text{total}}$. It can be noted that the scatter is very small; most points lie near the regression line. The correlation coefficients for case G1 and G2 have been found in both situations. The highest correlation is 0.71 in G1 and 0.72 in G2. The regression line is shown in Figure 1(a–b) and was constructed using 200 points. The linear relation was calculated as

$$\text{Dst} = (-0.035) + (-5.36)B_{\text{total}} \quad \text{for G1},$$
$$\text{Dst} = (-0.03) + (-7.39)B_{\text{total}} \quad \text{for G2}.$$

Figure 1(c) shows the IMF (maximum peak of $B_{\text{total}}$) versus the Dst minimum. In this figure, a linear correlation between $B_{\text{total}}$ and the Dst can be seen in the G3 case, i.e. the strength of the GMS strongly depends on the total magnetic field $B_{\text{total}}$. The correlation coefficient is found to be reasonably high; as shown in Table 2, it is $-0.80$. When solar wind flows within the interplanetary medium, it can interact with IMF structures and is controlled by the total magnetic field $B_{\text{total}}$. In the present study, it is observed that $B_{\text{total}}$ is reasonably high during the GMSs in all three cases.

We found a linear relation between $B_{total}$ and Dst. Therefore, $B_{total}$ is a good indicator of GMSs. For prediction, we derived a linear relation between the maximum value of $B_{total}$ and the Dst, given by $Dst = (-0.016) + (-5.39)B_{total}$.

## 3.2 The $z$ Component of IMF ($B_z$) vs. Dst

The solar wind carries with it the magnetic field of the Sun with an intensity $\sim 5$ nT. This magnetic field or IMF has a northward or southward orientation. If the IMF is directed southward, $B_z$ is negative and the pressure is raised (due to coronal mass ejections or solar flares), then a GMS can be expected. It is generally believed that the GMSs are triggered by $B_z$, which are southward IMFs. It has been verified by Mansilla (2008) that GMS intensity correlates well with the southward component $B_z$ of the IMF better than the density and solar wind velocity. However, the idea that the IMF $B_z$ component is essential for determining magnetospheric activity is not new. These results were confirmed by Kane & Echer (2007), in which they suggested that for intense storms, a larger negative value of $B_z$ gives a larger negative value of Dst. In another study, the statistical results between the different geomagnetic indices (Kp, Dst, AE) and IMF $B_z$ from 1964 to 2010 have been carried out by Shi et al. (2012). The correlation coefficient may only give us a brief description of the relationship between IMF $B_z$ and the geomagnetic indices, which shows that when IMF $B_z$ is southward, the geomagnetic activities become active. The following formula has been obtained for the different ranges of $B_z$.

$$
\begin{aligned}
Dst &= 6.5 + 6.8B_z\,, & cc &= 0.98 & \text{when} && -20 < B_z < 0\,, \\
Dst &= -8.1 + 0.3B_z\,, & cc &= 0.79 & \text{when} && 0 < B_z < 10\,, \\
Dst &= 22.7 - 2.7B_z\,, & cc &= -0.68 & \text{when} && 10 < B_z < 25\,.
\end{aligned}
$$
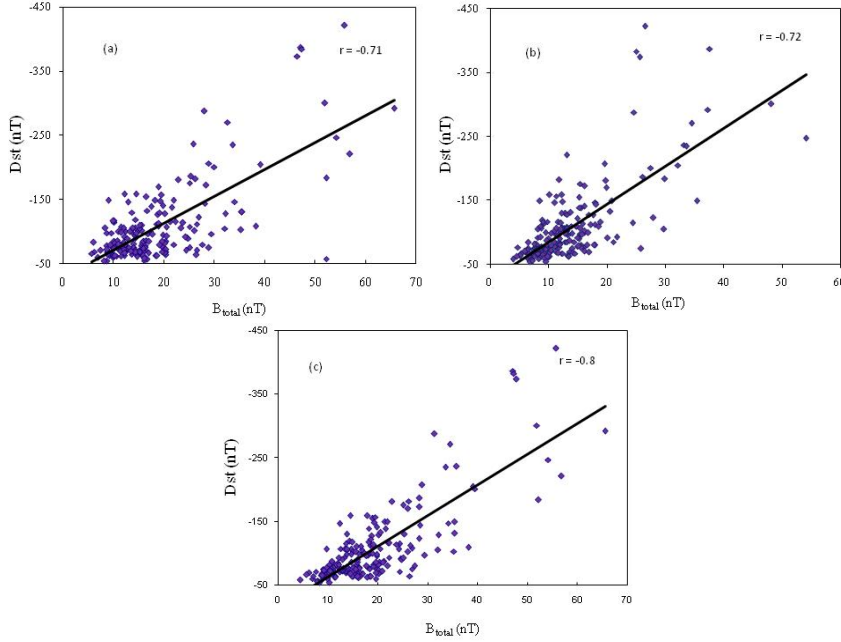


**Fig. 1** (a) The IMF vs. the Dst minimum for G1. (b) The IMF vs. the Dst minimum for G2. (c) The IMF vs. the Dst minimum for G3.

From the above discussion, we adopted a new approach for study, which has been described in the previous section. It has been taken from the statistical analysis for three different instants during the storm in the present study.

Figure 2(a–c) shows the Dst and the corresponding value of the $z$ component of the IMF $B_z$ for all three situations: (i) at the time of IP shock when the total magnetic field of the IMF suddenly changes, (ii) at the instant of the Dst minimum, and (iii) the maximum value of southward directed $B_z$ for all 200 events during GMSs.

Here we discuss the first two conditions G1 and G2. The first one is when the solar wind interacts with Earth's magnetic field at the initial point and induces the magnetic storms, which is known as the initial phase of GMSs. The second one, when a magnetic storm reaches its peak value, is called the main phase of the storm. Figure 2(a–b) shows a plot of Dst versus the corresponding values of the $B_z$ component of the IMF. It is noted that in the previously reported work, researchers only focused on the southward turning of $B_z$, but in the present work, we have considered both southward and northward orientations of $B_z$. In the figures, the scatter of points is large and large $B_z$ values are associated with a wide range of Dst values in both cases. This indicates two possibilities: there may be some relationship between Dst and the southward direction of $B_z$ or there may be some relation between Dst and the northward directed $B_z$. Southward and northward turning of $B_z$ with Dst are shown in Figure 2(a–b) for both cases. The correlation has been calculated for both cases G1 and G2. The highest correlation in the range Dst $\leq -50$ nT is 0.22 for both G1 and G2. According to previous studies, the strength of the GMS strongly depends on the southward component $B_z$. But in the present study, the correlation coefficient has been found to be low, where $r = 0.22$ in the first two cases. It is concluded that in the present study, the solar wind's southward turning of $B_z$ has significant growth, mainly after the initial phase and before the main phase of a GMS, but not during the main phase, which is tested here. The absence of a highly linear correlation between $B_z$ and Dst during the main phase as well as the initial phase does not mean that the southward turning of the $B_z$ component is not a geoeffective parameter. It is observed from the first two cases that a time delay has been found between the Dst minimum and the southward $B_z$ maximum. The correlation is weak due to the time delay. It has been observed that a weaker magnetic reconnection also occurred with a northward orientation of the $B_z$. Generally, moderate storms are produced due to the northward turning of $B_z$. It is clearly seen from Figure 2(a–b) that the regression lines show a positive relation towards a higher value of the southward turning of $B_z$. The regression relation has been calculated for both conditions, as given below

$$\text{Dst} = (-0.51) + (2.76)B_z \qquad \text{for G1} ,$$
$$\text{Dst} = (-0.378) + (9.105)B_z \quad \text{for G2} .$$

It is also noteworthy that in Figure 2(a–b) the southwards direction of $B_z$ is more dependable than the northward $B_z$ for the initial and main phases. Furthermore, it is observed that some GMSs are induced due to the northward turning of $B_z$ and sometimes it starts with the northward turning. However, only moderate storms were observed to have a northward direction for $B_z$. In Figure 2(a–b), the regression line indicates that the southward component plays an important role in GMSs. In order to solve this problem, we have taken the maximum value of southward directed $B_z$ with respect to the Dst, as shown in Figure 2(c). The correlation coefficient has been found to be reasonably high; as shown in Table 2, the value of $r$ is 0.82. Hence, the correlation indicates a fairly good relationship between Dst and the southward directed $B_z$ of IMF for the G3 condition. Thus, the magnitude of the magnetic field and its duration play very important roles in the generation of a magnetic storm. Therefore, the orientation of the IMF carried by the solar wind plays an important role in geomagnetic activity. It is well established that the southward $B_z$ component of the IMF has the most important influence on the magnetosphere and the high latitude ionosphere as it controls the fraction of energy in the solar wind, which is extracted by the magnetosphere. When the southward $B_z$ is strongly negative, then the magnetic reconnection between the IMF and the geomagnetic field
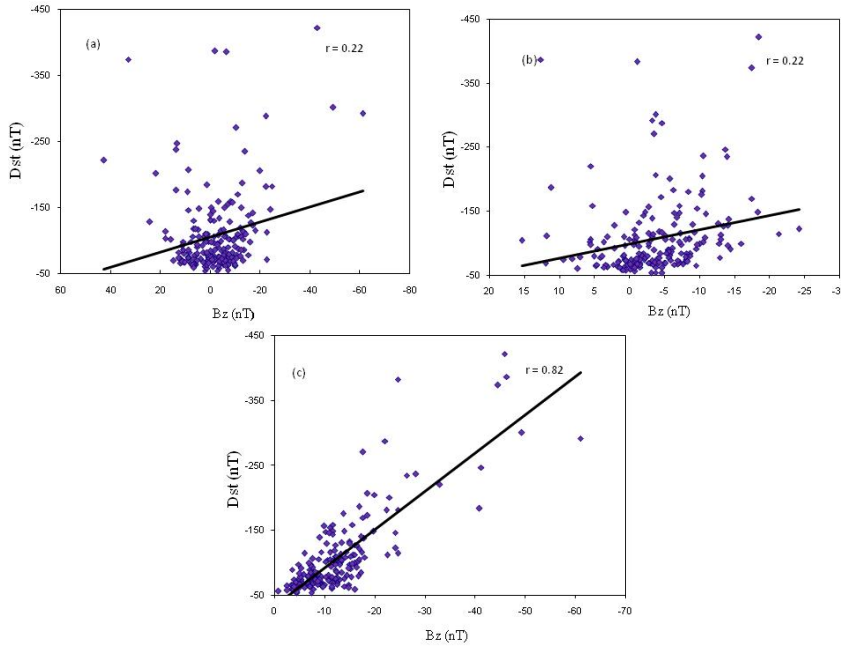
**Fig. 2** (a) The $B_z$ ($z$ component of IMF) vs. the Dst minimum for G1. (b) The $B_z$ ($z$ component of IMF) vs. the Dst minimum for G2. (c) The $B_z$ ($z$ component of IMF) vs. the Dst minimum for G3.

produces open field lines that allow mass, energy and momentum to be transferred from the solar wind to the Earth's magnetosphere. Gonzalez et al. (1994) and Gonzalez et al. (1999) have also suggested that the primary causes of magnetic storms are intense ($>10$ nT) and long duration ($>3$ h) conditions for a southward IMF. Therefore, it is convenient to suggest that the southward IMF is an essential interplanetary requirement needed to activate the magnetic reconnection.

In the present study, it is observed that the southward $B_z$ component of the IMF is an important factor for GMSs during cycle 23. However, it is also observed that sometimes northward $B_z$ components are also responsible for moderate storms. Accordingly, the intensity of storms depends on the magnitude of southward $B_z$. The intensity of storms will be higher when the negative $B_z$ is directed more southward. It has been observed that in the present study, the magnitude of $B_z$ is neither maximum during the initial phase (at the instant of IP shock) nor during the main phase (at the instant of Dst minimum). It has been seen in this study that there is a time delay between the maximum value of southward $B_z$ and the Dst minimum and, further, that this time delay can be used in the prediction of the intensity of a magnetic storm, two-three hours in advance of the main phase of a GMS. A linear relationship has been derived between the maximum value of the southward directed $B_z$ and the Dst for prediction, which is given by

$$\text{Dst} = (-0.06) + (7.65)B_z .$$

### 3.3 The $y$ Component of IMF $B(B_y)$ vs. Dst

Recent observations show that the steady stream of solar particles and energy from the Sun, known as the solar wind, can enter the magnetosphere more easily than previously thought. In general, the solar wind's ability to penetrate into near Earth space is thought to rely on the magnetic alignment of the IMF. As the solar wind streams from the Sun toward the dayside of Earth, its magnetic fields

connect up to those of Earth, resulting in a sudden and dramatic reconfiguration or reconnection of the field lines. This is most efficient when the IMF is aligned southward – opposite to the northward alignment of Earth's magnetic field. The temporary tangling of the field lines creates ideal conditions for magnetic reconnection, allowing large amounts of plasma and magnetic energy to be transferred from the solar wind to the magnetosphere. Magnetic reconnection also occurs more weakly with a northward orientation of the IMF, which is generally only seen at higher latitudes. Spacecraft observations have indicated that Kelvin-Helmholtz waves may play an important role in the transfer of solar wind material into the magnetosphere during a northward IMF – a hypothesis bolstered by the fact that the waves can facilitate magnetic reconnection. However, previous identification of Kelvin-Helmholtz waves during the northward IMF was limited to the low latitude flanks of the magnetosphere. These new observations have shown that there are numerous regions of transient formation, which enable the continuous reconnection process. This can also sometimes occur in the absence of any strong solar feature. The team of scientists from the CLUSTER mission has now directly observed these Kelvin-Helmholtz waves at high latitudes under other orientations of the IMF (Hwang et al. 2012). Instead of pointing north or south, the IMF was pointing west, down towards the Earth. Under these conditions, the CLUSTER data showed waves on the duskside of the high-latitude magnetopause. The magnetopause is the boundary between the relatively undisturbed magnetosphere and the magnetosheath, the region containing solar wind plasma that has come across the bow shock that protects Earth from the direct onslaught of solar wind plasma. These scientists were also able to characterize how differences in IMF orientation greatly influenced the Kelvin-Helmholtz waves because of variations in the thickness and other characteristics of the boundary layer (Hwang et al. 2012).

A study was also conducted by Zhao & Zong (2012) after analyzing 42 years of IMF and geo-magnetic indices data and 1270 storm sudden commencement events from 1968 to 2010 by defining the GMS Russell-McPherron effect (R-M effect) (Zhao & Zong 2012) with a positive/negative IMF $B_y$. The results obtained in this study have shown that the response of geomagnetic activity to the GMS R-M effect with positive/negative IMF $B_y$ is rather profound: geomagnetic activity is much more intense around the autumnal equinox when the direction of the IMF is away from the Sun, and it is also much more intense around the vernal equinox when the direction of the IMF is toward the Sun.

In order to solve this problem, a statistical analysis is performed, the result of which is plotted in Figure 3(a–c). It shows the Dst and the corresponding value of the $y$ component of IMF $B_y$ (east-west direction) for all three predefined conditions G1, G2 and G3.

Figure 3(a–b) shows the Dst and the corresponding value of the $B_y$ component of IMF $\boldsymbol{B}$. The $B_y$ component shows the east-west direction of the IMF. The correlations have been calculated for the first two cases (G1, G2). The highest correlation is $-0.07$ in G1 and $-0.16$ in G2. The regression equations are shown by solid lines, which are constructed by using 200 points and given as

$$\mathrm{Dst} \;=\; (-0.48) + (-2.61)B_y \quad \text{for G1}\,,$$

$$\mathrm{Dst} \;=\; (-1.06) + (-2.66)B_y \quad \text{for G2}\,.$$

The correlation is found to be very poor for both G1 and G2 conditions. It is very clear from these figures that during IP shock and the main phase, the eastward and westward components of the IMF are less geoeffective. According to new experimental findings, the $B_y$ may also be the cause of GMSs and hence we have calculated the value of the $B_y$ maximum with the Dst minimum during the storms. Figure 3(c) presents the $B_y$ of the IMF (maximum peak of $B_y$ for all 200 events) versus the Dst minimum. In this figure, the observed correlation is low between $B_y$ and Dst in the G3 case, i.e. the strength of the GMS is not strongly dependent on the $B_y$. The correlation coefficient of $-0.42$ has been found to be reasonable, which is shown in Table 2. When solar wind flows within the IP medium, it can interact with IMF structures and is controlled by the total magnetic field
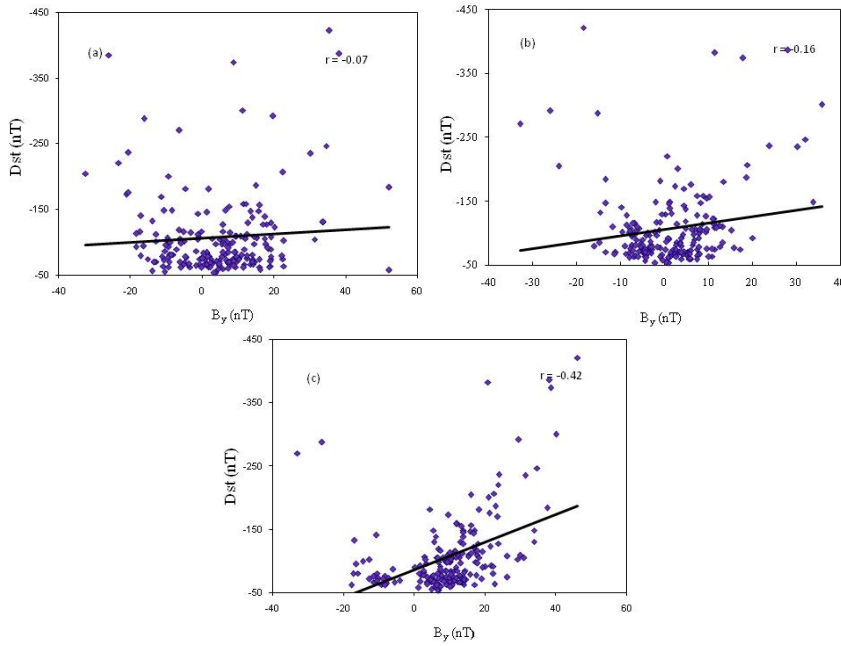
**Fig. 3** (a) The $B_y$ ($y$ component of the magnetic field $B$ which shows an east-west direction) vs. the Dst minimum for G1. (b) The $B_y$ ($y$ component of magnetic field $B$ which shows an east-west direction) vs. the Dst minimum for G2. (c) The $B_y$ ($y$ component of the magnetic field $B$ which shows an east-west direction) vs. the Dst minimum for G3.

$B_{\text{total}}$. It is generally believed that the GMSs are triggered by $B_z$, which are southward IMFs. When this southward component of the IMF reconnects with the northward directed geomagnetic field at the dayside of the magnetopause, the energy is transported from the solar wind into the magnetosphere. However, the present statistical analysis shows that the $B_y$ components of the IMF are also an important parameter for energy transportation from the solar wind to the magnetosphere. For predicting GMSs or the strength of storms we derived a linear relation between the maximum value of $B_y$ and the Dst, as given below

$$\text{Dst} = (-0.25) + (-5.76)B_y .$$

### 3.4 Speed of Solar Wind ($V$) vs. Dst

The solar-terrestrial relationship includes the effect of solar output and its variations. It also includes propagation effects in the IP medium, which ultimately produce disturbances in the geomagnetic field. As such, the near-Earth IP plasma and fields are expected to have a direct relationship with geomagnetic disturbance indices. *In situ* measurements of the IMF and solar wind parameters began in late 1962 and now cover more than four solar cycles by Dwivedi et al. (2010). The observations have helped in establishing several useful statistical relationships between the indices of geomagnetic activity and the causative parameters including solar wind speed ($V$) (Snyder et al. 1963). The data have also been examined for their long-term variability in terms of the eleven-year solar cycle component (Feldman et al. 1978; King 1979; Bieber et al. 1993). From early observations of the solar wind bulk speed, Snyder et al. (1963) were able to establish its close correlation with the geomagnetic disturbance index Kp. Crooker et al. (1977) showed that when long-term averages

(covering a duration of six months or more) are considered, the correlation between geomagnetic activity and solar wind speed is indeed very striking. Soon after the data for solar wind parameters became available, Snyder et al. (1963) reported a good correlation between the solar wind velocity ($V$) and the geomagnetic index Kp. Possible IP mechanisms for the creation of very intense GMSs are discussed in detail by Gonzalez et al. (1999). However, for the long-term averages of solar wind, the effects of individual storms are temporary and only steady-state characteristics prevail. Even though Crooker & Gringauz (1993) had initially reported a high correlation between solar wind speed and geomagnetic activity, later results reported a low correlation for the years after 1976. For solar cycles 20, 21 and 22 (1964–1995), Kane (1997) found that the correlation between solar wind velocity and aa index (similar to Ap index) is +0.91±0.02 for cycle 20 and +0.77±0.04 for cycle 21, but only +0.73±0.04 for cycle 22 (a decreasing trend), indicating that some other factors are needed to adequately describe the relationship with the aa or Ap indices.

Through the above discussion, we have concluded that the correlation between $V$ and magnetic indices like Kp and Ap are very good for intense GMSs. But in the present study, we have considered the correlation between speed $V$ and Dst indices for Dst $\leq -50$ nT during cycle 23. Figure 4(a–c) shows Dst and the corresponding value of the speed of solar wind plasma in three different situations: (i) at the instant of IP shock, (ii) at the instant of Dst minimum, and (iii) the maximum value of solar wind speed $V$ for all 200 events during GMSs.

The correlations have been calculated for three different situations (G1, G2 and G3) and are shown in Figure 4(a–c). The linear trend indicated by the thick line plots the regression equation.

Figure 4(a–b) shows the plot of Dst vs. speed $V$. It can be seen that the scatter is small; most of the points in the scatterplot lie near a fixed range of speed for Dst $\leq -50$ nT, indicating correlations of $-0.35$ for G1 and $-0.24$ for G2. It has been observed that the correlation is poor in both cases. The regression relation represented below is constructed using 200 points.

$$\text{Dst} = (-0.012) + (-0.198)V \quad \text{for G1} \,,$$

$$\text{Dst} = (-0.008) + (-0.196)V \quad \text{for G2} \,.$$

In Figure 4(c), the correlation ($r$) for the overall range is found to be $-0.40$. However, if the two giant events on 2003 November 20 (Dst $= -422$) and 2003 October 29 (Dst $= -383$) are removed, the scatter is small and most points lie near a small area representing a range of speeds and are concentrated near the average value, with a wide range of velocities varying between 400 and 900 km s$^{-1}$. The more intense GMSs are not associated with large values of solar wind velocities. The correlations for all selected ranges are below 0.50. According to Kane (1997), a moderate or
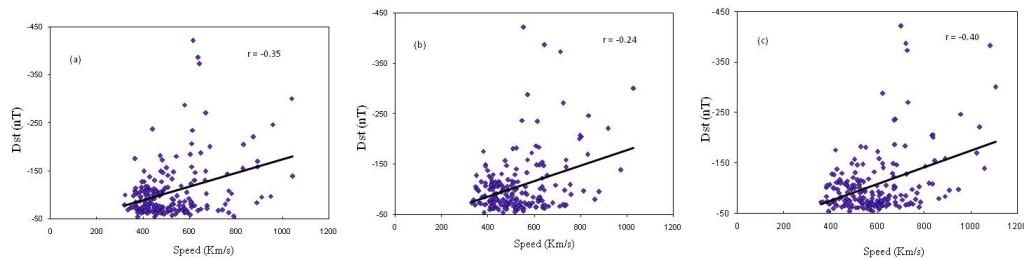


**Fig. 4** (a) The solar wind speed ($V$) vs. the Dst minimum at the instant of the IP shock, defined as G1. (b) The solar wind speed ($V$) vs. the Dst minimum at the instant of the IP shock, defined as G2. (c) Maximum peak values of the solar wind speed ($V$) vs. the Dst minimum during GMSs, defined as G3.
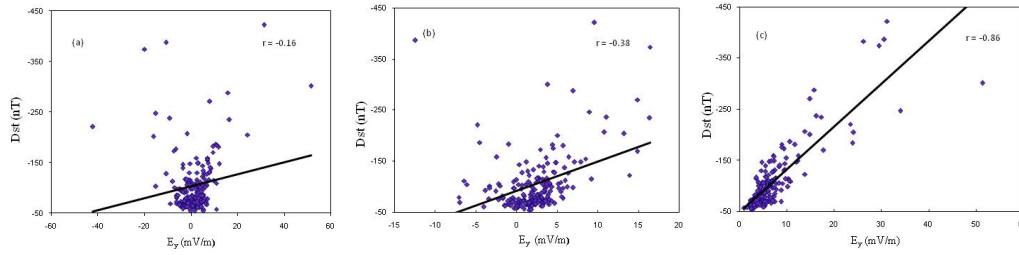
**Fig. 5** (a) The relationship between the electric field strength $E_y$ vs. the Dst minimum for G1. (b) The relationship between the electric field strength $E_y$ vs. the Dst minimum for G2. (c) The relationship between the electric field strength $E_y$ vs. the Dst minimum for G3.

intense GMS only occurs when the value of speed exceeds $\sim 350$ km s$^{-1}$. Thus, the Dst-$V$ relationship is moderate and agrees with the previous results. This indicates a reasonable relationship between Dst and $V$ for moderate storms. The present study does not agree with the previous results in that there is a linear relation between the speed of the solar wind and GMSs. It is found in the present and previous studies that the speed of solar wind is an important factor to initiate a GMS, but on the basis of the present study, we conclude that most of the storms are induced by the average value of speed. When the value of speed is 350 to 750 km s$^{-1}$, most of the storms are produced. Hence, with average growth in the speed of solar wind, we can also predict the arrival of magnetic storms but cannot forecast their strength. A linear relation between the maximum value of solar wind speed $V$ and the Dst has been derived as

$$\text{Dst} = (-0.002) + (-0.18)V.$$

### 3.5 Electric Field ($E_y$) vs. Dst

In their study, Dwivedi et al. (2010) calculated statistical results over a long period of time, which demonstrate that the most effective parameter for producing large-scale geomagnetic disturbances is the total IP electric field or, in other words, it is the product of $V$ and $B$ during the years 1965-2007. The statistical analysis carried out by Dwivedi et al. (2010) has concluded that $VB$ is the most effective parameter in producing large scale disturbances in the geomagnetic field. They observed that neither $V$ nor $B$ is very effective in inducing geomagnetic disturbances; rather, it is the combined effects of $B$ and $V$ together which are rather effective in producing large-scale geomagnetic disturbances. In a statistical study, Yue & Zong (2011) demonstrated that a perpendicular shock would result in more intense geomagnetic activity than a parallel one, because a perpendicular shock front could compress the IMF more effectively than a parallel one. The result shows that 74% of intense (Dst $\leq -100$ nT) and 69% of super (Dst $\leq -200$ nT) GMSs are related to a negative IMF $B_z$ precondition. To confirm this result, the possibility of using modern techniques of direct data analysis is being explored.

Figure 5(a–c) shows Dst and the corresponding value of $E_y$ for three different situations: (i) at the instant of the IP shock (ii) at the instant of the Dst minimum, and (iii) the maximum value of $E_y$ for all 200 events during GMSs. From the critical observations shown in Figure 4(c), it can be inferred that there is some saturation effect of fast solar wind on GMSs (Dst is not keeping up with larger solar wind speeds).

However, the product of $V$ and $B_z$ is also an effective parameter to initiate the GMSs. The product of $V$ and $B_z$ gives the electric current $\boldsymbol{E_y} = -\boldsymbol{V} \times \boldsymbol{B_z}$. We have analyzed the effect of $E_y$ on GMSs. The correlations for the first two cases (G1 and G2) are shown in Figure 5(a–b). The highest correlation is –0.16 for G1 and –0.38 for G2. The regression equation is shown by a solid line.

The regression line has been constructed by using 200 points in the case $\text{Dst} = (-0.56) + (3.87)E_y$ for G1 and $\text{Dst} = (-0.34) + (-16.28)E_y$ for G2. Figure 5(c) presents the maximum value of $E_y$ versus the Dst minimum. A linear relation between $E_y$ and Dst can be seen in the case of G3, i.e. the strength of the GMS is strongly dependent on $E_y$. The correlation coefficient is reasonably high, –0.86, when solar wind flows within the IP medium.

First, we will discuss G1 and G2. Figure 5(a–b) shows plots of Dst vs. $E_y$ for hourly average values during 1996-2007 for cases G1 and G2. The scatter is moderate in both cases and correlation coefficients are low in both cases, therefore, results do not agree with the previous result in which only the southward turning of $B_z$ is taken into account. In particular, the significance of $\boldsymbol{V} \times \boldsymbol{B_z}$ only takes into account the reconnection for negative $B_z$ of IMF. Correlations are found to be low, similar to the $B_z$ component of IMF, because in these figures, we have taken both positive and negative $B_z$ (the southward direction as well as the northward direction). It is shown in the figures that GMSs occurred due to both the southward and northward direction of $B_z$ but the regression line shows that the highly intense GMS occurred due to the southward direction of $B_z$. Only moderate storms occurred due to the northward direction of $B_z$. Furthermore, Figure 5(c) shows that the Dst minimum corresponds to the maximum peak of $E_y$ with the southwards $B_z$ component of only the IMF. The correlation between $E_y$ and the Dst maximum is found to be –0.86.

The correlations were also calculated for different Dst ranges (50–100, 100–200, 200–300 and $\geq 300$) and are plotted in Figure 5(c). The correlation for all selected ranges was also considered. The range $-100 \leq \text{Dst} \leq -50$ has the highest correlation of –0.56, the range $-200 \leq \text{Dst} \leq -100$ has the highest correlation of $-0.58$ and the range $-300 \leq \text{Dst} \leq -200$ has the highest correlation of 0.05 while $\text{Dst} \leq -300$ nT has the highest correlation of 0.85. The overall correlation has increased to 0.86 for $\text{Dst} \leq -50$ nT. Thus, not only $V$ but the product of $VB_z$ is a better representative of the Dst. In this study, it is observed that $E_y$ is also an important factor for GMSs as a southward $B_z$ component of IMF. It is further observed that the magnitude of $E_y$ is neither maximum during the initial phase nor during the main phase, therefore, there is a phase difference between the peak value of $E_y$ and the Dst minimum. It is also observed that the peak of $E_y$ has been raised before the main phase of GMSs, similar to the southwards $B_z$. This time delay can be used in the prediction of the strength of GMSs, two to three hours before the main phase of GMSs. In the present study, we found a linear relation with $E_y$ so we calculated the equation for the linear regression line describing Dst which is given as $\text{Dst} = (-0.57) + (1.04)E_y$.

### 3.6 Pressure (nPa) vs. Dst

Based on the size of the Earth's magnetosphere and the observed case where its magnetopause is pushed inward and outward by changing solar wind conditions, it has been suggested that dynamic pressure is the main solar wind driver, rather than the orientation of the IMF (Southwood & Kivelson 2001; Cowley & Bunce 2003). The size of the terrestrial magnetosphere is determined by the balance between the solar wind dynamic pressure and the pressure exerted by the magnetosphere, principally in that its magnetic field is responsible for the shape of the magnetosphere. This drag is predominantly caused by the mechanism known as reconnection, in which the magnetic field of the solar wind is linked to the magnetic field of the magnetosphere.

It is well known that the Dst index is sensitive to the solar wind dynamic pressure variations. The present corrected Dst index is the pressure-corrected Dst index, which is corrected by removing the effects of the solar wind pressure and the quiet time ring current.

$$\text{Dst}^* = \text{Dst} - b\sqrt{P} + c,$$

where $\text{Dst}^*$ is the corrected Dst index and $P$ is the solar wind dynamic pressure.

The southward IMF precondition and intensified southward MF within the shock/sheath region, together with shocked solar wind, would produce a larger ring current injection function $Q(VB_s)$,

and thus a larger GMS (Dst index) according to the Burton equations (Burton et al. 1975)

$$\frac{d\mathrm{Dst}}{dt} = Q(VB_s) - \frac{\mathrm{Dst}}{\tau(VB_s)} \ .$$

Here $B_s$ is the southward IMF, $V$ is the solar wind velocity and $t(VB_s)$ is the timescale of the ring current.

To study the effect of dynamic pressure on GMSs, we have taken three situations which are depicted in Figure 6(a–c). Figure 6(a–c) shows the Dst and the corresponding value of solar wind pressure for three different situations defined earlier. Figure 6(a–b) shows the Dst and the corresponding values of dynamic pressure. It is noted that the scatter is small in Figure 6(a, b), and most of the points lie near the regression line. Correlations for the first two cases (G1, G2) have been calculated and are shown in Figures 6(a–b). The highest correlation is –0.30 for G1 and –0.48 for G2 and the regression equation is shown by the solid line. The regression line has been constructed by using all the 200 points, and the equation is Dst $= (-0.26) + (-8.63)P$ for G1 and Dst $= (-0.23) + (-14.67)P$ for G2. At the instant of the IP shock, the correlation between pressure (nPa) and Dst minimum is low but the average line shows a linear relation between them, similar to Figure 6(b). We have taken the maximum value of pressure vs. Dst minimum during the storms. Figure 6(c) presents the IP magnetic pressure versus the Dst minimum. In this figure, a linear correlation between Pressure (nPa) and Dst can be seen for the G3 case; the correlation coefficient has been found to be good. It is –0.50, i.e. the strength of the GMS is strongly dependent on pressure. For the prediction, we derived a linear relation between the maximum value of solar wind pressure (nPa) and Dst to be

$$\mathrm{Dst} = (-0.15) + (-7.0)P.$$

Several combinations were tried in order to ascertain the dependence of the geomagnetic indices on the parameters of solar wind in the IP medium during events in solar cycle 23. The most promising candidate is found in the form of solar wind pressure. Figure 6 shows the dependency of the Dst on the solar wind pressure. Figure 6(c) shows the best-fit line, i.e. it indicates that most observations from cycle 23 follow a linear relationship between Dst and the solar wind pressure (nPa).

### 3.7 Density vs. Dst

Khabarova et al. (2006) proposed that the minimum Dst value during the main phase may be successfully derived from the maximum value of solar wind density before the onset of a storm, the minimum IMF $B_z$ value during the GMS, and the time lag between the density maximum and the $B_z$ minimum. Different from the previously mentioned material, a simple conclusion could be of
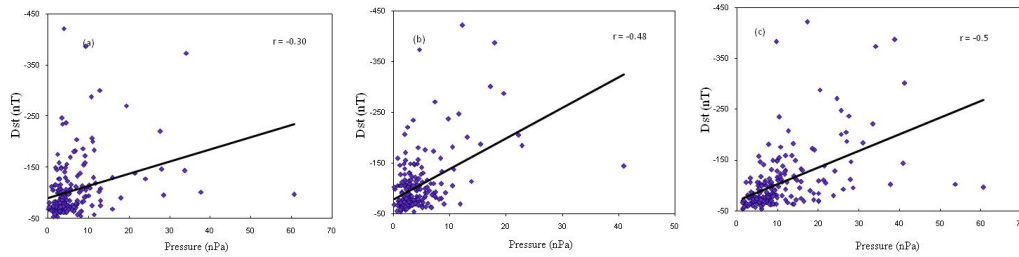


**Fig. 6** (a) The Dst and corresponding values of solar wind pressure at the instant of the IP shock. (b) The Dst and corresponding values of solar wind pressure at the instant of the Dst minimum. (c) The Dst and corresponding maximum values of dynamic pressure for all 200 events during GMSs.

practical use in space weather forecasting. Using information about the solar wind from the ACE spacecraft, it could be possible to estimate the strength of a GMS at least one hour in advance and take necessary precautions.

Figure 7(a–c) shows the Dst and the corresponding value of solar wind density in three predefined situations: (i) at the instant of the IP shock, (ii) at the instant of Dst minimum, and (iii) the maximum value of density during storms. It was noted that the scatter is very large in all three cases; but most points lie near the regression line. The correlation for cases (G1, G2) have been calculated and is shown in Figure 7(a–b).

The highest correlation is –0.14 in G1 and –0.24 in G2, which is shown by regression lines. The regression lines constructed using 200 points are given as below

$$\mathrm{Dst} = (6.43) + (-118.4)N \qquad \text{for G1},$$
$$\mathrm{Dst} = (-0.201) + (-8.32)N \qquad \text{for G2}.$$

Figure 7(c) shows the proton density versus the Dst minimum (negative) for G3. No definite relationship between both parameters is found. It can be seen from this figure that greater intensities of GMSs are not necessarily associated with high values of solar wind density. This means that there is a high probability that the intensity of a GMS is not determined by increased density. The correlation coefficient between both parameters is –0.31 for G3. A linear relation between the maximum value of density $N$ and Dst is achieved by $\mathrm{Dst} = (-0.12) + (-3.94)N$. It is clear that the proton density is not a geoeffective parameter, but charged particles still enter Earth's atmosphere during the storm and produce substorms.

### 3.8 Temperature vs. Dst

In addition, due to academic interest in how magnetized plasma behaves, it is important to study the solar wind's interaction with the magnetosphere. This interaction controls space weather phenomena. The ability to develop an accurate space weather forecast depends very much on the forecaster having a good understanding of how the magnetosphere works, i.e. having a correct paradigm. Empiricism alone is unlikely to produce accurate predictive models. It is known that during solar activity, i.e. CMEs and solar flare eruptions, hot plasma ejects from the Sun with a temperature of a million degrees Kelvin and flows into the IP medium in the form of solar wind, so it may be possible to relate the solar wind temperature to the Dst.

In order to understand this problem, we have plotted Figure 8(a–c) to show the Dst and the corresponding value of solar wind temperature in three different situations of GMSs: (i) at the instant of the IP shock, G1 (ii) at the instant of the Dst minimum, G2, and (iii) the maximum value of temperature during GMSs, G3.
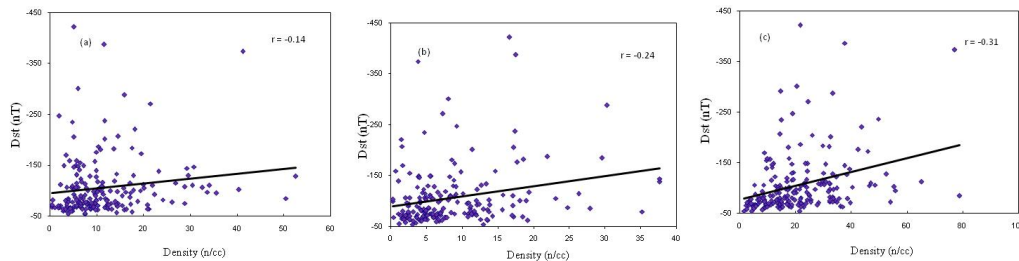


**Fig. 7**  (a) The proton density vs. the Dst minimum for G1. (b) The proton density vs. the Dst minimum for G2. (c) The proton density vs. the Dst minimum for G3.
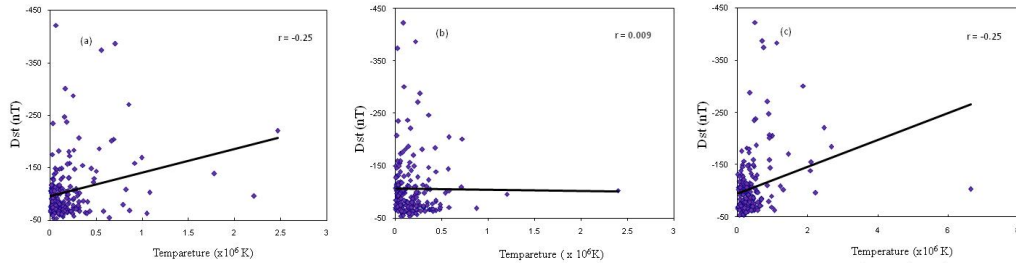
**Fig. 8** (a) Dst variation with temperature for G1. (b) Dst variation with temperature for G2. (c) Dst variation with temperature for G3.

First, we discuss the two cases G1 and G2; therefore, we have checked the temperature profile from the beginning to the peak of a storm. Figure 8(a–b) shows the Dst and the corresponding value of temperature for G1 and G2. It can be noted that the scatter is very small; most points lie towards the low temperature range. The correlation coefficient for G1 and G2 has been calculated, and is reported in Table 2. The highest correlation is –0.251 for G1 and 0.009 for G2 and the solid line in these figures plots the regression equation. The regression equation constructed using the plotted points is $\mathrm{Dst} = (1.46) + (-1.84 \times 10^{-3})T$ for G1 and $\mathrm{Dst} = (-0.53) + (-1.0948 \times 10^{-6})T$ for G2. In both cases, it is observed that the correlation is very poor between both parameters. Later we have taken the maximum values of the temperature during storms for the G3 condition, which are shown in Figure 8(c). This shows the solar wind temperature versus the Dst minimum. In this figure, a correlation between temperature and Dst can be seen in the G3 case to be weak between the plasma temperature and the Dst, i.e. the solar wind temperature can have a large range but most of the event occurs at a temperature less than 0.5 million Kelvin ($0.5 \times 10^6$ K). It is clearly seen in Figure 8(c) that the intense and severe storms can be produced at a low plasma temperature. For predicting a storm, we have derived a linear relation between the maximum value of plasma temperature ($T$) and the geomagnetic index Dst, which is given as

$$\mathrm{Dst} = (2.17) + (-0.1 \times 10^{-3})T \, .$$

### 3.9 Plasma $\beta$ vs. Dst

The plasma $\beta$ is defined as the ratio between the thermal pressure and the magnetic pressure of the plasma, which is of the order of 0.0001–0.1. Within the Sun's interior, the value of plasma $\beta \gg 1$, i.e. the thermal pressure of plasma is more dominating within the Sun's atmosphere but outside the Sun's atmosphere, in the interstellar medium plasma, $\beta \ll 1$, i.e. the magnetic pressure is more than the thermal pressure.

Figure 9(a–c) shows the Dst and the corresponding value of plasma $\beta$ for three different situations: (i) at the instant of the IP shock, (ii) at the instant of Dst minimum, and (iii) the minimum value of plasma $\beta$. Figure 9(a–c) shows the Dst and the corresponding value of plasma $\beta$. It can be noted that the scatter is small in all three cases, but most points lie near the low value of plasma $\beta$. The correlations for the first two cases (G1, G2) are 0.13 in G1 and 0.24 in G2 and the regression equation is shown by the solid line. The regression lines are constructed using 200 points, and have equations $\mathrm{Dst} = (-0.28) + (-96.93)\beta$ for G1 and $\mathrm{Dst} = (-0.978) + (-63.96)\beta$ for G2. A weak correlation has been found in the first two cases, but it is very clear from the regression lines that intense storms occurred during conditions when plasma $\beta$ was low. A negative correlation has been found with plasma $\beta$, i.e. most of the storms occurred during conditions when plasma $\beta$ was low. In this case, we have taken the minimum value of plasma $\beta$ with respect to the Dst during the storms.
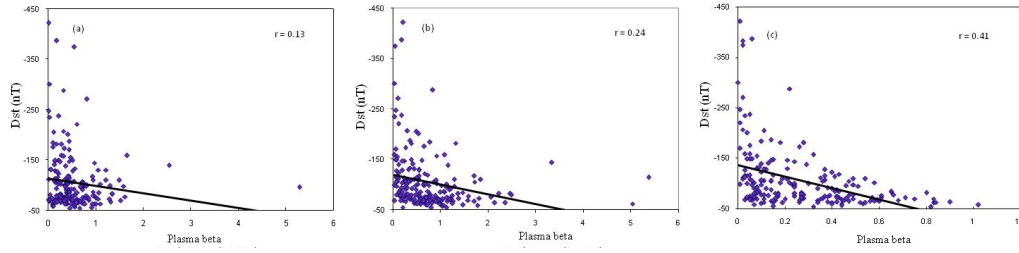
**Fig. 9** (a) Dst and the corresponding value of plasma $\beta$ at the instant of the IP shock. (b) Dst and the corresponding value of plasma $\beta$ at the instant of Dst minimum. (c) Dst and the corresponding minimum value of plasma $\beta$.

Figure 9(c) depicts the plasma $\beta$ versus the Dst minimum (negative) for G3. The correlation coefficient between both these parameters is 0.41 for G3. An ordinary correlation has been found. It can be seen that the GMSs with a greater intensity are not necessarily associated with high values of plasma $\beta$. This means that there is a high probability that the intensity of a GMS is not determined by the increased plasma $\beta$. In general, GMSs occurred when the plasma $\beta$ was low. We derived a linear relation between the minimum value of plasma $\beta$ and the Dst which is given as

$$\text{Dst} = (-0.27) + (-205.8)\beta\,.$$

This result confirmed our earlier findings: southward $B_z$ is a possible cause of GMSs at low plasma temperature. It is also confirmed that the plasma $\beta$ should be low during storm conditions. It also agrees with the Khabarova et al. (2006) study, which found the value of plasma $\beta$ is high before and after the storm.

## 4 CONCLUSIONS AND MODEL

We have used solar and IP data to find our conclusions. Analyses and observations are presented in the present paper. Based on the analysis done in previous sections, we have summarized our important conclusions as follows:

(1) It is observed that in the present study, $B_{\text{total}}$ is reasonably high during GMSs; therefore, we have found a linear relation between $B_{\text{total}}$ and the Dst. Therefore, $B_{\text{total}}$ is a good indicator of GMSs.

(2) It is observed in the present study that the southward $B_z$ component of the IMF is an important factor for GMSs during cycle 23. But in this study, it is also observed that sometimes northward $B_z$ components are also responsible for moderate storms. According to this study, the intensity of storms depends on the magnitude of southward $B_z$. Therefore, the intensity of storms will be as high as the negative southward $B_z$ is. A result of the study is that the magnitude of $B_z$ is neither maximum during the initial phase (at the instant of the IP shock) nor during the main phase (at the instant of the Dst minimum). So, it is seen in this study that there is a time delay between the maximum value of the southward $B_z$ and the Dst minimum and this time delay can be used in the prediction of the intensity of a magnetic storm two-three hours before the main phase of a GMS. A linear relation has been derived between the maximum value of the southward component of $B_z$ and Dst for prediction, which is $\text{Dst} = (-0.06) + (7.65)B_z$.

(3) When solar wind flows within the IP medium, it can interact with IMF structures and is controlled by the total magnetic field $B_{\text{total}}$. It is generally believed that the GMSs are triggered by $B_z$, southward IMFs. When this southward component of the IMF reconnects with the northward directed geomagnetic field at the dayside of the magnetopause, the energy is transported

from the solar wind into the magnetosphere. However, the present statistical analysis shows that the $B_y$ components of the IMF is also an important parameter for energy transportation from the solar wind to the magnetosphere.

(4) This indicates a reasonable relationship exists between the Dst and speed $V$ for a moderate storm. Consequently, the present study does not agree with previous results that there is a linear relation between the speed of solar wind and GMSs. In the present study, it has been seen that the speed of the solar wind is an important factor in the induction of a GMS but from the present study, we can conclude that most of storms are induced by solar wind with the average value of speed. When the value of speed is 350 km s$^{-1}$ to 750 km s$^{-1}$ most storms are produced. So, with average growth in the speed of the solar wind, we can only predict the arrival of a magnetic storm but we cannot forecast its strength.

(5) In this study, it is observed that $E_y$ is also an important factor for GMSs during cycle 23 in addition to the southward $B_z$ component of the IMF. It is also observed that the magnitude of $E_y$ is maximum neither during the initial phase nor during the main phase; therefore, there is a phase difference between the peak value of $E_y$ and the Dst minimum. This time delay can be used in the prediction of strength of GMSs, two-three hours before the main phase of a GMS. In the present study, we found a linear relation with $E_y$, so we also calculated the linear regression equation for Dst, which is Dst $= (-0.57) + (1.04)E_y$.

(6) To ascertain the dependence of geomagnetic indices on the parameters of the solar wind interacting with the IP medium during events in solar cycle 23, several combinations are tried. The most promising candidate is found in the form of solar wind pressure. The study shows this dependence on Dst. This study shows the best fit line, which indicates that most of the observations from cycle 23 show a linear relationship between Dst and the solar wind pressure (nPa).

(7) It is clear from the above discussion that the proton density is not a geoeffective parameter, but that charged particles enter Earth's atmosphere during a storm and produce substorms.

(8) A weak correlation has been found between plasma temperature and Dst, i.e. the solar wind temperature can have a large range but most of the events occur at a temperature less than 0.5 million K ($0.5 \times 10^6$ K). It is clear in the present study that intense and severe storms can be produced at low plasma temperature.

(9) This result confirms our earlier finding, that the southward $B_z$ is a possible cause of GMS at low plasma temperature. It is also confirms that the plasma $\beta$ should be low during storm conditions. It is also in good agreement with studies by Khabarova et al. According to their work, the value of plasma $\beta$ is high before and after a storm.

(10) The current paradigm of solar wind geoeffectiveness is as follows: for GMSs, the solar wind speed and the IMF intensity must be substantially higher than their 'average' values; the field must also be southwardly directed for a substantial length of time, and temperature and plasma $\beta$ should be low.

## 4.1 Space Weather Prediction Model

Space weather prediction involves forecasting the time of commencement of a GMS, based on solar and IP observations. Most of the currently used prediction methods are based on the formula of Burton et al. (1975). They are generally reliable, even though they depend solely on IP parameters, viz. the solar wind speed and the southward component of the IMF. However, when solar inputs are used for prediction, one encounters the problem of 'false alarms' (when the predicted events never occur) and of 'missing alarms' (when there are no obvious solar signatures of the GMS) as also reported by Schwenn et al. (2005). Although the presently available prediction schemes accurately predict the Dst index of the GMS, their prior warnings are a few hours ahead of the commencement of the GMS. This is because they are based on *in situ* properties of the solar wind that can be measured close to the Earth. For example, measurements from the ACE spacecraft give about 30 to

60 minutes of warning time as it measures properties of the solar wind at the Lagrangian point L1. However, the main drawback of all existing models is that they are only used for intense and super storms, so no model is available for all ranges of GMSs.

In the present paper we have developed a model for the prediction of GMSs and their strength. With the help of this model we can predict all categories of GMSs. This model is based on the following facts.

– The total IMF $B_{\text{total}}$ can be used as an alarm for GMSs. When there are sudden changes in total magnetic field $B_{\text{total}}$, this is the first warning that the conditions are present for a storm's arrival.
– It is observed in the present study that the southward $B_z$ component of the IMF is an important factor for GMSs during cycle 23. The result of this study shows that the magnitude of $B_z$ is maximum neither during the initial phase (at the instant of the IP shock) nor during the main phase (at the instant of Dst minimum). Hence, it is seen in this study that there is a time delay between the maximum value of the southward $B_z$ and the Dst minimum and that this time delay can be used in the prediction of the intensity of a magnetic storm two to three hours before the main phase of a GMS. A linear relation has been derived between the maximum value of the southward component of $B_z$ and the Dst for prediction, which is

$$\text{Dst} = (-0.06) + (7.65)B_z\,. \tag{1}$$

After testing Equation (1), we have observed that the duration of the southward turning of $B_z$ is also an important factor for the induction of GMSs; then after including the time duration of the southward $B_z$, this result becomes more accurate. So, after adding time $t$ of the southward $B_z$, the equation becomes

$$\text{Dst} = (-0.06) + (7.65)B_z + t\,, \tag{2}$$

where $t$ is the time of the southward turning of $B_z$.

Some auxiliary conditions should be fulfilled with this equation: the speed of the solar wind should be on average 350 km s$^{-1}$ to 750 km s$^{-1}$, plasma $\beta$ should be low and most importantly, the plasma temperature should be low for intense storms. If the plasma temperature is less than $0.5 \times 10^6$ K then the Dst value will be greater than the predicted value of the Dst or if the temperature is greater than $0.5 \times 10^6$ K then the Dst value will be less (some nT) than the value predicted given by Equation (2).

## References

Akasofu, S.-I. 1983, Space Sci. Rev., 34, 173

Bieber, J. W., Chen, J., Matthaeus, W. H., Smith, C. W., & Pomerantz, M. A. 1993, J. Geophys. Res., 98, 3585

Burton, R. K., McPherron, R. L., & Russell, C. T. 1975, J. Geophys. Res., 80, 4204

Cowley, S. W. H., & Bunce, E. J. 2003, Planet. Space Sci., 51, 57

Crooker, N. U., Feynman, J., & Gosling, J. T. 1977, J. Geophys. Res., 82, 1933

Crooker, N. U., & Gringauz, K. I. 1993, J. Geophys. Res., 98, 59

Dungey, J. W. 1961, Physical Review Letters, 6, 47

Dwivedi, V. C., Pandey, V. S., Tiwari, D. P., & Agrawal, S. P. 2010, Indian Journal of Radio & Space Physics, 39, 252

Feldman, W. C., Asbridge, J. R., Bame, S. J., & Gosling, J. T. 1978, J. Geophys. Res., 83, 2177

Gonzalez, W. D., Joselyn, J. A., Kamide, Y., et al. 1994, J. Geophys. Res., 99, 5771

Gonzalez, W. D., Tsurutani, B. T., & Clúa de Gonzalez, A. L. 1999, Space Sci. Rev., 88, 529

Hwang, K.-J., Goldstein, M. L., Kuznetsova, M. M., et al. 2012, Journal of Geophysical Research (Space Physics), 117, A08233

Joselyn, J. A., & McIntosh, P. S. 1981, J. Geophys. Res., 86, 4555

Kane, R. P. 1997, in Annales Geophysicae, 15, 1581 (Springer)

Kane, R. P., & Echer, E. 2007, Journal of Atmospheric and Solar-Terrestrial Physics, 69, 1009

Khabarova, O., Pilipenko, V., Engebretson, M. J., & Rudenchik, E. 2006, in Proc. Int. Conf. Substorms-8 (Banff Centre, Canada), 127

King, J. H. 1979, J. Geophys. Res., 84, 5938

Lakhina, G. S. 1994, Surveys in Geophysics, 15, 703

Lindsay, G. M., Russell, C. T., Luhmann, J. G., & Gazis, P. 1994, J. Geophys. Res., 99, 11

Mansilla, G. A. 2008, Physica Scripta, 78, 045902

Shi, X. F., Zong, Q. G., & Wang, Y. F. 2012, Science China Technological Sciences, 55, 2769

Snyder, C. W., Neugebauer, M., & Rao, U. R. 1963, J. Geophys. Res., 68, 6361

Southwood, D. J., & Kivelson, M. G. 2001, J. Geophys. Res., 106, 6123

Sugiura, M. 1964, in Annals of the International Geophysics Year, 35, 945 (Oxford: Pergamon Press)

Yue, C., & Zong, Q. 2011, Journal of Geophysical Research (Space Physics), 116, A12201

Zhao, H., & Zong, Q.-G. 2012, Journal of Geophysical Research (Space Physics), 117, A11222